Biochemical Pharmacology 79 (2010) 1141–1148

Contents lists available at ScienceDirect

Biochemical Pharmacology

journal homepage: www.elsevier.com/locate/biochempharm

The isothiocyanate produced from glucomoringin inhibits NF-kB and reduces myeloma growth in nude mice *in vivo*

Dario Brunelli [a,*], Michele Tavecchio [a], Cristiano Falcioni [a], Roberta Frapolli [a], Eugenio Erba [a], Renato Iori [b], Patrick Rollin [c], Jessica Barillari [b], Carla Manzotti [d], Paolo Morazzoni [d], Maurizio D'Incalci [a]

[a] *Laboratory of Cancer Pharmacology, Department of Oncology, Istituto di Ricerche Farmacologiche Mario Negri, Via La Masa 19, 20156 Milano, Italy*
[b] *Agricultural Research Council, Research Center for Industrial Crops (CRA-CIN), Via di Corticella 133, 40129 Bologna, Italy*
[c] *Institut de Chimie Organique et Analytique UMR-CNRS 6005, Université d'Orléans, B.P. 6759, F-45067 Orleans Cedex 2, France*
[d] *Indena S.p.A., Viale Ortles 12, 20139 Milano, Italy*

ARTICLE INFO

Article history:
Received 20 October 2009
Received in revised form 4 December 2009
Accepted 7 December 2009

Keywords:
Isothiocyanate
Glucosinolate
Myeloma
NF-kB
Sulforaphane

ABSTRACT

Glucosinolates (GLs), natural compounds extracted from *Brassicaceae* and precursors of isothiocyanates (ITCs), have been studied in the last decades mostly due to their chemopreventive activity and, more recently, for their potential use as novel chemotherapeutics. The aim of the present study was to investigate the *in vitro* and *in vivo* activity of glucomoringin (GMG), an uncommon member of the GLs family, and to compare it with glucoraphanin (GRA), one of the most studied GL. We have evaluated the potency of both compounds in inducing cell death, cell cycle perturbations, apoptosis, NF-kB inhibition and GST-π activity in human carcinoma cells with different GST-π contents as well as in human multiple myeloma and leukaemia cell lines. GMG-derived ITC (GMG-ITC) showed to be more effective compared to GRA-derived ITC (Sulforaphane), especially in inhibiting NF-kB activity and inducing apoptosis through a caspase-dependent pathway; these effects were more pronounced in myeloma cells, in which we could also observe a long lasting growth inhibitory effect, probably due to NF-kB inhibition, which is considered essential for myeloma cell survival. Both GLs were able to induce cell death in the μM range in all tested cell lines but caused cell cycle perturbations only in myeloma cells; they were also able to modulate the GST/GSH pathway by causing a 3-fold increase in GST-π activity in MCF7 cells. *In vivo* study showed that pure GMG-ITC was only slightly active in a carcinoma mice model, whereas it had significant antitumoral activity in a myeloma model, causing little toxicity.

1. Introduction

Vegetables are important sources of compounds with cancer chemopreventive activity [1,2]. Among them are isothiocyanates (ITCs), species generated in *Brassicaceae* such as broccoli, Brussels sprouts and cauliflower, and they have attracted a lot of research interest as modulators of tumor growth since the original observation by Sidransky et al. [3]. In vegetables, ITCs are stored in the form of inactive precursors called glucosinolates (GLs) and can be released after tissue damage by enzymatic hydrolysis involving myrosinase (MYR, E.C. 1.2.1.147), a thioglucoside glucohydrolase that is physically separated from GLs under normal conditions [4,5]. As the intestinal microflora of mammals, including humans, possess myrosinase-like activity, GLs can also be converted into ITCs in the mammalian digestive tract [6,7]. ITCs have been reported to inhibit tumor growth in different preclinical *in vivo* studies [8–10]. Moreover, epidemiological studies have shown an inverse relationship between dietary consumption of *Brassicaceae* and risk of developing lung, breast and colon cancer [11–13]. ITCs have many effects through which they may exert their protective action against cancer progression: they can induce phase-2 drug metabolizing enzymes like glutathione-S-transferase (GST) and quinone-reductase (QR) [14–17] through a Nrf-2 pathway, cause cell cycle arrest and apoptosis [18–20] and inhibit phase-I drug metabolizing enzymes and NF-kB related genes [20–22]. Sulforaphane (4-methylsulfinylbutyl isothiocyanate) is an ITC which has been extensively studied in recent years, as it was found to possess cancer chemopreventive and chemotherapeutic properties in a variety of preclinical models [9,13,22]. Glucomoringin (GMG) (4(alpha-L-rhamnosyloxy)-benzyl isothiocyanate) is an atypical GL due to the presence of a second saccharide residue in the aglycon side chain which might confer biological properties on the GL scaffold which are distinctly different from those of other members of the family (Fig. 1). In the light of the putative role of sulforaphane and other ITCs [8] in cancer management, we wanted to characterize potential cancer chemotherapeutic properties of

* Corresponding author. Tel.: +39 02 39014239; fax: +39 02 39014734.
E-mail address: brunelli@marionegri.it (D. Brunelli).

0006-2952/$ – see front matter © 2009 Elsevier Inc. All rights reserved.
doi:10.1016/j.bcp.2009.12.008

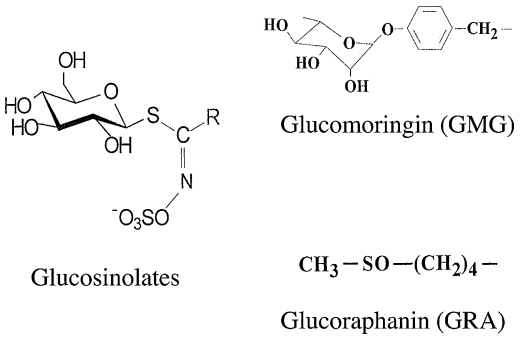

Fig. 1. Chemical structures of glucosinolates and GMG and GRA side chains.

GMG-ITC. The cytotoxicity, cell cycle phase perturbation, GST activity modulation, NF-kB regulation, apoptosis induction and caspase activation induced by myrosinase-activated GMG (MA-GMG) were investigated *in vitro* in various carcinoma, leukaemia and myeloma cell lines and compared with those of sulforaphane generated from glucoraphanin (MA-GRA). Finally, since the *in vitro* studies revealed a much greater potency of MA-GMG on myeloma cells compared to both leukemia and carcinoma cells, chemically purified GMG-ITC was also tested in a preliminary *in vivo* study comparing its anti-neoplastic activity in mice bearing either human myeloma or carcinoma in order to confirm the increased efficacy on myelomas and to address its potential as a novel chemotherapeutic.

2. Materials and methods

2.1. Isolation and purification of compounds

GMG and GRA were isolated respectively from *Moringa oleifera* L. (fam. *Moringaceae*) and *Brassica oleracea* L. (fam. *Brassicaceae*; var. *acephala*; subvar. *laciniata*) seeds. Both GLs were purified in two sequential steps, by anion exchange and size exclusion chromatography, according to previously reported methods [23,24]. Individual GLs were characterised by ^{1}H and ^{13}C NMR spectrometry and the purity was assayed by HPLC analysis of the desulfo-derivative according to the ISO 9167-1 method (EEC Regulation No. 1864/90 Enclosure VIII. Offic. Eur. Commun. L170: 27-34) resulting about 99% based on peak area value, but about 90–92% on weight basis due to their high hygroscopic properties. The enzyme MYR was isolated from seeds of *Sinapis alba* L. according to a reported method [25] with some modifications. The stock solution used in the present study had a specific activity of ~60 units/mg of soluble protein and was kept at 4 °C after dilution in H_2O at 34 U/ml. One MYR unit was defined as the amount of enzyme able to hydrolyse 1 μmol/min of sinigrin at pH 6.5 and 37 °C. the MYR solution was stored at 4 °C in sterile distilled water until use. GLs were dissolved in H_2O at a concentration of 1 mM, and kept at −20 °C. Just before use, the solutions were diluted in medium at the desired concentration. In every treatment made 5 μl of MYR for every 1.5 ml of GLs solutions were added in order to produce the active ITCs. GMG-ITC was produced via MYR catalyzed hydrolysis of GMG, performed in 0.1 M phosphate buffer pH 6.5 at 37 °C. The total conversion of pure GMG into GMG-ITC was confirmed by HPLC analysis of the desulfo-derivative (EEC Regulation No. 1864/90 Enclosure VIII. Offic. Eur. Commun. L170: 27-34), which allowed us to monitor the reduction until complete disappearance of GMG in the reaction mixture. Acetonitrile was then added to the mixture until the final concentration was 20% and GMG-ITC was purified by reverse-phase chromatography, which was performed using a HR 16/10 column packed with LiChrospher RP-C18 (MERCK), connected to a GradiFrac System (Pharmacia). After washing with acetonitrile 20%, elution was carried out with a gradient up to 60% acetonitrile. Fractions were collected and analysed using a Hewlett-Packard Model 1100 HPLC system with an Inertsil ODS3 column (250 mm × 3 mm, 5 mm). Chromatography was performed with 1 mL/min flow rate at 30 °C by eluting with a linear gradient of water (A) and acetonitrile (B) from 30% B to 80% in 20 min. Elution of GMG-ITC was detected by a diode array, monitoring the absorbance at 229 nm. Fractions containing GMG-ITC (peak purity > 99%) were collected, the solvent were removed by concentration in a rotary evaporator, and the final solution was freeze-dried. The GMG-ITC was characterized and unambiguously identified by ^{1}H and ^{13}C NMR and mass spectrometry techniques.

2.2. Drugs, cells culture condition and experimental tumor models

The human ovarian cancer cell line A2780, the human NSCLC (non-small cell lung cancer) H460 WT and its sub-line H460 S5 were grown in RPMI 1640 medium (Cambrex, Bio Science, Verviers, Belgium) containing 10% fetal bovine serum (FBS) (Sigma–Aldrich Co. Ltd., UK), 1% (v/v) 200 mM L-glutamine (Cambrex). H460 S5 cell line was derived from the parental line transfected by calcium-phosphate method with pCDNA3 (Invitrogen, Carlsbad, CA, USA), containing an insert coding for the antisense sequence of the GST-π protein; this line was maintained in selection by adding 5 μl/ml of G418 (100 mg/ml). The human mammarian cancer cell lines MCF7 π and NEO were grown in DMEM medium (Cambrex) containing 10% fetal bovine serum (FBS), 1% (v/v) 200 mM L-glutamine, 1% Sodium Pyruvate 100 mM (Cambrex) and 1% MEM non essential amino acid solution 100× (Cambrex); both cell lines were maintained in selection by adding 5 μl/ml of G418 (100 mg/ml). MCF7 π cell line was derived from wild type cells transfected with a plasmid containing an insert coding for the GST-π protein while MCF7 NEO cell line was transfected with an empty plasmid. RAW-NFkB, a murine immortalized macrophage cell-line, stably transfected with the luciferase gene put under a promoter responsive only to NFkB, was grown in RPMI-1640 medium with 10% inactivated FBS (HyClone, UT, USA) and 1% (v/v) L-glutamine (200 mM). The human myeloid myeloma cell line RPMI-8226 was maintained in RPMI-1640 medium with 10% inactivated FBS and 1% (v/v) L-glutamine (200 mM). The human myeloid leukaemia cell line HL60 was maintained in RPMI-1640 medium with 10% inactivated FBS and 1% (v/v) L-glutamine (200 mM). All cell lines were kept at 37 °C in a humidified 5% CO_2 atmosphere in T-25-cm^2 tissue culture flasks (IWAKI, Bibby Sterilin, Staffordshire, UK). All cell lines used are stable immortalized cancer cell lines and experiments were performed with cells not exceeding 30 passages. For *in vivo* studies 4–6-week-old female CD1 *nu/nu* mice (Charles River, Calco, Lecco, Italy) and 5-week-old male SCID mice were used. Mice were maintained under specific pathogen-free conditions, and provided food and water *ad libitum*. Procedures involving animals and their care are conducted in conformity with the institutional guidelines that are in compliance with national (D.Ln.116, G.U., Suppl. 40, 18 Febbraio 1992, Circolare No. 8, G.U., 14 Luglio 1994) and international laws and police (EEC Council Directive 86/609, OJ L 358, 1, Dec. 12, 1987; Guide for the Use of Laboratory Animals, United State National Research Council, 1996). Human ovarian A2780 cancer cells (8×10^6 cell/mouse) and human myeloma RPMI8226 cancer cells (30×10^6 cell/mouse) were implanted s.c. into the flank of recipient mice. When tumor was palpable (mean tumor weight value for the groups was 100–150 mg for the RPMI8226 bearing mice and 50–100 mg for the A2780 bearing mice respectively), animals were divided randomly into test groups consisting of 6–8 mice each, according to Geran et al. Tumor growth was measured every two days using a calliper. GMG-ITC

was dissolved in H_2O:Tween 5% and drug solutions were prepared every day before treatments; mice were treated i.p. daily, 5 days a week for 2–3 weeks with 20 mg/kg of GMG-ITC.

2.3. Flow cytometric DNA cell cycle analysis

Exponentially growing cells were treated for 24 h with different concentration of myrosinase-activated-GLs. At the end of treatment and at different time intervals after drug-washout the cells were counted by a Coulter Counter Channelyzer 256 (Beckman Coulter) and fixed in 70% cold ethanol and kept at 4 °C. The cells were washed with cold PBS and stained with a 1 ml solution containing 5 μg/ml propidium iodide in PBS and 12.5 μl/ml RNase 1% in water overnight in the dark. Flow cytometric cell cycle analysis were performed on at least 20,000 cells by using FACS Calibur instrument (Becton Dickinson, Sunnyvale, CA, USA). Fluorescence pulses were detected using a laser beam at 488 nM and a band pass filter 620 ± 35 nm, for red fluorescence, in combination with a dichroic mirror at 570 nm. [26].

Percentages of distribution of cells in the phases of the cell cycles were analyzed according to the method by Bertuzzi et al. [27].

2.4. Cell death

Apoptosis was evaluated by two different methods: TUNEL Assay and Caspase-3 activation. TUNEL assay was performed following this protocol: at the end of treatment, and at different time intervals after drug washout, the cells were fixed in 70% ethanol and kept at 4 °C before staining. The fixed cells were washed in cold PBS and permeabilized with 0.25% Triton X-100 (Sigma) in PBS for 5 min in ice. After removing Triton X-100, cells were incubated in 50 μl of solution containing terminal-dUTP-trasferase (TdT) and FITC-conjugated dUTP deoxynucleotides 1:1 in storage buffer (Boehringer Mannheim, Germany) for 90 min at 37 °C in the dark. Caspase-3 activation was assessed by fixing cells in 1% paraformaldehyde for 1 h in ice and, subsequently, in 70% ethanol. Cells were washed in PBS and permeabilized for 10 min with 0.004% saponin in PBS supplemented with 0.5% BSA and 5 mM EDTA. After centrifugation cells were resuspended with 20 μl of anti-active caspase-3 direct PE-antibody (BD Biosciences, Pharmingen, Canada) for 1 h in the dark. Flow cytometric analysis were performed on at least 20,000 cells by using FACS Calibur instrument. Fluorescence pulses were detected using a laser beam at 488 nM and a band pass filter 530 ± 25 nm for FITC fluorescence and 585 ± 45 nm for PE fluorescence.

2.5. Luciferase assay

For this assay we used a commercial kit (E1500, Promega, Madison, WI, USA). Briefly, RAW-NFkB cells were plated in 6 wells Petri at 150,000 cells/ml (2 ml/well) and 24 h later were treated with different concentrations of myrosinase-activated-GLs. After 24 h cells were washed with cold PBS and we added Passive Lysis Buffer (1×) for 10 min to lyse the membranes. The pellet was then collected, centrifuged, and supernatant kept at −20 °C. Proteins were quantified by a standard kit (BioRad, USA) and 20 μl were put in a round-bottom tube (Becton Dickinson, MA, USA). For every 25 μl of protein solution 50 μl of Luciferase Substrate were added and the samples were read with a Lumat LB 9057 (EG&G BERTHOLD) luminometer for 10 s.

2.6. NF-kB activity assay

This assay was performed using a commercial kit (EZ-DETECT NfkB p50 Transcription Factor Kit, PIERCE, Rockford, IL, USA) which, by using plates coated with specific NF-kB DNA consensus sequences to which only the active NF-kB complex can ligate, can minimize nonspecific binding. Exponentially growing RPMI-8226 cells were treated for 24 h with different concentrations of myrosinase-activated-GLs. After the end of the treatment and 24 h after drug washout cells were lysed using RIPA extraction buffer. The pellet was then collected, centrifuged, and supernatant kept at −20 °C. Proteins were quantified by a standard kit (BioRad). Proteins were subsequently utilized to detect NF-kB activity following manufacturer instructions.

2.7. GST-π activity assay

Exponentially growing MCF-7 cells were treated for 24 h with different concentration of myrosinase-activated-GLs. After treatment cells were scraped and resuspended in H_2O, sonicated and centrifuged and thereafter the supernatant was used to determine both protein concentration and GST activity. Prtoeins were quantified by a standard kit (BioRad, USA) and GST-π activity by monitoring the conjugation of glutathione with 1-cloro-2,4-dinitrobenzene (CDNB); briefly 100 μl of proteins were put in solution with 100 μl GSH 10mM, 100 μl Phospate Buffer, 680 μl H_2O and 20 μl CDNB 50 mM and the increase in the absorbance at 340 nm generated by the conjugation reaction was then followed for 1 minute using a spectrophotometer (UVIKRON-860, Kontron Instrument) and the results expressed as percentage of control activity.

3. Results

3.1. Growth inhibition and cell cycle effects

In preliminary studies exposure-efficacy conditions for MA-GMG and MA-GRA in various human carcinoma cell lines were optimised using the MTT assays (data not shown). The effects incremented by increasing the exposure time up for 24 h but only a modest increase was observed for 48 and 72 h exposures; 24 h treatment was, thus, considered as the optimal exposure time for the subsequent experiments. Due to the suggested role of the GST/GSH pathway in modulating ITCs citotoxicity [12,14,16], ability of both MA-GMG and MA-GRA to induce cell death was subsequently studied using cell count assays in two pairs of isogenic carcinoma cell systems with a 2-fold (H460 WT/S5) or 25-fold (MCF7 π/NEO) difference in GST-π content. MA-GMG showed an IC_{50} range of 18–29 μM while MA-GRA was slighty less potent with a range of 19–30 μM (Table 1). A small increase in potency of both compounds was present in the H460 S5 cell line compared to its WT counterpart but, on the other hand, no differences could be observed in the MCF7 model thus suggesting that this is probably not a major determinant in GCs cytotoxicity. To evaluate whether growth inhibition was associated with an alteration in cell cycle phase distribution, we also performed flow cytometric DNA cell cycle analysis on all the four cell lines. The ITCs did not cause any significant alteration in cell cycle phases distribution (data not shown).

Table 1
IC_{50} values on different cell lines after 24 h treatments with different concentrations of MA-GM or MA-GRA; IC_{50} values were calculated 48 h after drug washout. Data are mean values of at least 3 experiments each consisting of 3 replicates.

Cell line	IC_{50} (μM)	
	MA-GMG	MA-GRA
H460 WT	29.07 ± 0.76	29.35 ± 0.49
H460 S5	18.50 ± 6.65	19.10 ± 0.92
MCF7 π	21.08 ± 5.67	27.33 ± 3.85
MCF7 NEO	19.76 ± 4.38	25.59 ± 4.21

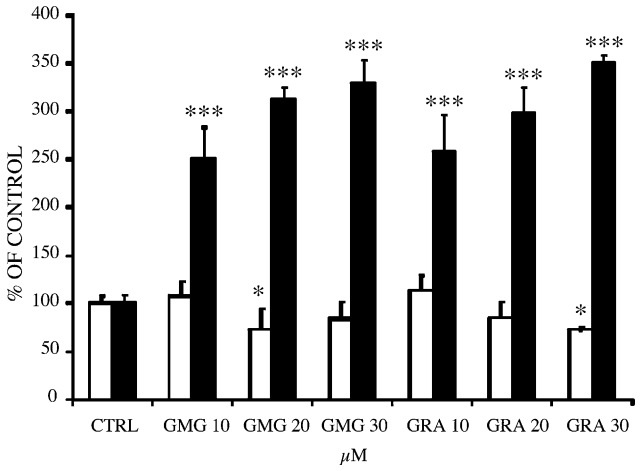

Fig. 2. GST-π activity in MCF7 π (white columns) and MCF7 NEO (black columns) cells evaluated after 24 h MA-GMG or MA-GRA treatment. Results are shown as percentage of relative controls. Error bars represent the standard deviation. Statistical analysis: $^{*}p < 0.01$, $^{**}p < 0.005$, $^{***}p < 0.001$ compared with untreated controls.

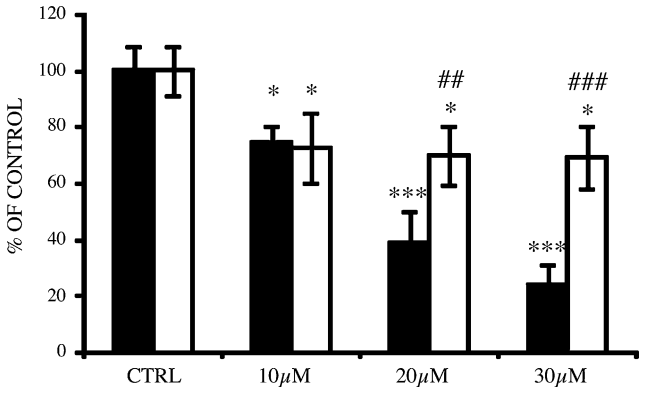

Fig. 3. NF-kB-dependent luciferase expression in RAW NF-kB after 24 h treatment with MA-GMG (black columns) or MA-GRA (white columns). Data shown are mean values of 3 experiments each consisting of 3 replicates. Error bars represent the standard deviation. Statistical analysis: $^{*}p < 0.01$, $^{**}p < 0.005$, $^{***}p < 0.001$ compared with untreated controls. $^{\#}p < 0.01$, $^{\#\#}p < 0.005$, $^{\#\#\#}p < 0.01$ compared with MA-GMG treatments.

3.2. Effects on GST-π activity

To better understand the potential role of the GST/GSH pathway in ITCs mechanism of action, we evaluated the effects of MA-GMG and MA-GRA on GST-π activity using the isogenic cell lines MCF7 NEO and MCF7 π: this model was preferred to the H460 one due to the increased differences in basal GST-π activity between the two cell lines thus permitting a more sensitive and accurate measurement of the effects. Enzymatic activity was measured 24 h after ITCs treatment and results are shown in Fig. 2. Both compounds induced GST-π activity in MCF7 NEO cells by 2.5–3.5-fold, whilst there was no significant induction in the MCF7 π line. Various studies [28,29] have related the growth-modulating activity of ITCs to their ability to deplete cellular GSH, thus rendering cells vulnerable to oxidative stress and apoptotic signalling. To explore whether the cytotoxic effect of MA-GMG and MA-GRA might have been caused by GSH depletion, we exposed MCF7 π and NEO cells to MA-GMG and MA-GRA after pre-treatment with the GSH-depleting agent BSO (buthionine sulfoximine). Pre-treatment with BSO failed to modify significantly the cytotoxic potential of either compound (results not shown).

3.3. Effects on NF-kB dependent gene expression

The transcription factor NF-kB is responsible for many cellular signalling pathways and changes in NF-kB-dependent gene regulation is often associated with tumorigenesis. In the light of the NFkB-inhibiting properties of sulforaphane [21,22] we studied the effects of MA-GMG and MA-GRA on NF-kB in RAW NF-kB cells. MA-GMG inhibited NF-kB activity, expressed as luciferase level, in a dose-dependent manner (Fig. 3). Maximal inhibition (by 70%) was observed at 30 μM. In contrast MA-GRA did not depress NFkB activity by more than 30%. Since the survival of many human myeloma cell lines seems to be exquisitely sensitive towards alterations in NF-kB related pathways [30–32], we decided to further investigate the ability of MA-GMG or MA-GRA to inhibit NF-kB using the human multiple myeloma cell line RPMI-8226. Fig. 4 shows NF-kB activity at the end of treatment with MA-GMG or MA-GRA and 24 h after drug washout. MA-GMG inhibited NF-kB activity in these cells in a dose dependent manner at lower concentrations than those used in the experiments employing RAW NF-kB cells described above. The inhibitory effect of MA-GMG was maintained up to 24 h after drug washout, whilst that of MA-GRA was reversed after treatment. The importance of NF-kB inhibition in RPMI-8226 cell survival was further confirmed with the use of parthenolide and cynaropicrin, two previously reported NF-kB inhibitors, which showed comparable results with those obtained with ITCs and a very strong correlation between NF-kB inhibition and growth inhibition (Supplementary material).

3.4. Cell cycle perturbation and apoptosis induction on myelomas

Considering the NF-kB inhibition observed in the RPMI-8226 cell line even at low drug concentrations, we decided to further investigate the growth inhibitory and cell cycle perturbation effects of both MA-GMG and MA-GRA using this model. Fig. 5 shows that the growth inhibitory effect of both ITCs was 3–4 fold greater than those observed in carcinoma derived cell lines

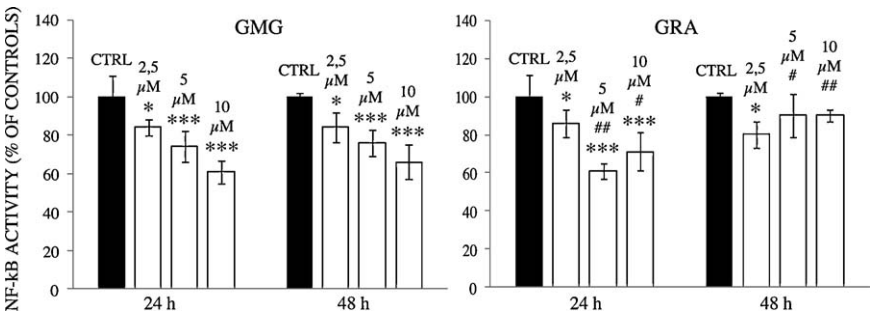

Fig. 4. NF-kB activity in RPMI-8226 cell line cell line evaluated after 24 h treatment with MA-GMG or MA-GRA and 24 h after drug washout. Data shown are mean values of 2 experiments each consisting of 3 replicates. Error bars represent the standard deviation. Statistical analysis: $^{*}p < 0.01$, $^{**}p < 0.005$, $^{***}p < 0.001$ compared with untreated controls. $^{\#}p < 0.01$, $^{\#\#}p < 0.005$, $^{\#\#\#}p < 0.01$ compared with MA-GMG treatments.

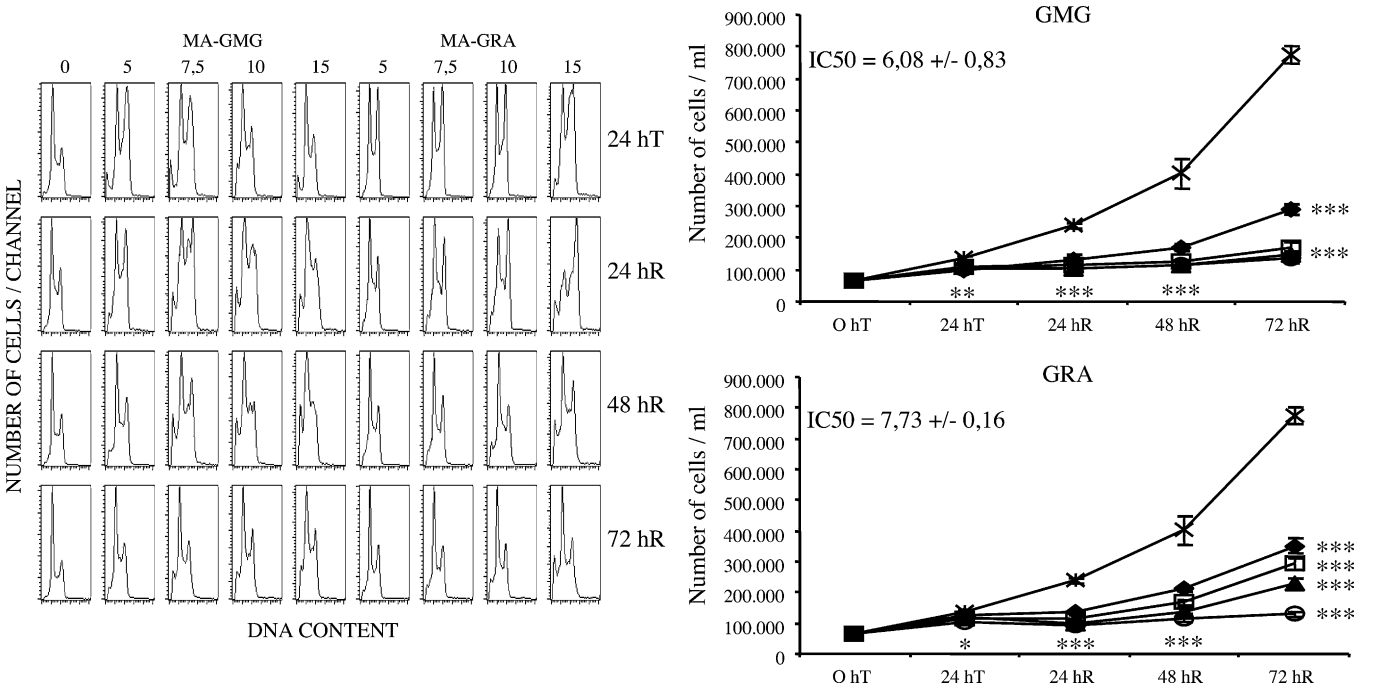

Fig. 5. Growth inhibitory effects (right) and cell cycle phase perturbations (left) induced on RPMI-8226 cell treated for 24 h with 0 (—✱—), 5 (—●—), 7.5 (—□—), 10 (—▲—) or 15 μM (—⊖—) of MA-GMG or MA-GRA. Error bars represent the standard deviation. IC_{50} values were calculated 48 h after drug washout. Statistical analysis: $^{*}p < 0.01$, $^{**}p < 0.005$, $^{***}p < 0.001$ compared with untreated controls.

Table 2
Percentage of cells in the various phases of the cell cycle after 24 h treatment with different concentrations of MA-GMG or MA-GRA and 24, 48 and 72 h after drug washout.

	CTRL	GMG 5	GMG 7.5	GMG 10	GMG 15	GRA 5	GRA 7.5	GRA 10	GRA 15	
% G1	30	20	23	30	32	20	20	21	19	24hT
% S	53	59	40	28	29	54	53	54	56	
% G2M	17	21	36	42	39	26	27	25	25	
% G1	33	20	18	19	25	21	20	20	10	24hR
% S	51	60	68	71	64	61	60	51	54	
% G2M	16	20	14	10	11	18	20	29	36	
% G1	30	26	24	26	40	25	25	25	19	48hR
% S	53	48	63	56	51	57	54	56	61	
% G2M	17	16	13	18	9	18	21	19	20	
% G1	34	22	22	24	25	23	24	27	26	72hR
% S	50	58	59	57	57	59	57	52	51	
% G2M	16	20	19	19	18	18	19	21	23	

reaching an IC_{50} of 6–7 μM and, most noticeably, it was correlated with a strong cell cycle perturbation mainly due to a G_2M phase block (Table 2). To address if the observed increase in sensitivity was due to the different nature of the myeloma cells compared to carcinoma-derived tumor cells, we performed the same experiments also on another myeloid-derived tumor which is typically quite sensitive to drug treatments, HL60; our results demonstrates that this was not the case since the IC_{50}s of 15–16 μM obtained with both drug treatments were comparable to those obtained in solid tumor cells (Fig. 6). It has been reported that GL-derived ITCs act as apoptotic inducers [18–20], thus we investigated this mechanism of cell death, once again, both on carcinoma-derived and myeloid-derived cell lines. After MA-GMG or MA-GRA exposure, H460 WT and H460 S5 cell lines showed no apoptosis induction (data not shown) and the same results were also obtained with HL60 cells (Fig. 7, right upper panel) while, on the other hand, both compounds induced apoptosis in RPMI-8226 cells (Fig. 7, left upper panel) and the percentage of apoptotic cells detected was higher after MA-GMG treatment. Apoptotic cells were already detectable after 6 h exposure (data not shown). With the aim of understanding whether the apoptotic process was caspase-3 dependent, we also marked cells with an anti-caspase antibody (Fig. 7, lower panel). The results showed a nearly perfect correlation between the percentages of apoptotic and caspase-3 activated cells for both the RPMI-8226 (lower left panel) and HL60 (lower right panel) suggesting that the caspase pathway is the main, if not the only, pathway involved in this apoptotic process.

3.5. GMG-ITC activity in experimental tumor mouse model

In order to evaluate its potential use as an antineoplastic agent against carcinomas or myelomas, GMG-ITC was administered to two different murine cancer models. In the first model, Swiss Ncr *nu*/*nu* mice bearing A2780 ovarian cancer were treated daily, 5 days a week, for 2 weeks with i.p. injections of either 20 mg/kg GMG-ITC or an equivalent volume of vehicle solution. Treated mice showed a reduced tumor growth (Fig. 8, upper panel), with the difference between the two groups becoming statistically signifi-

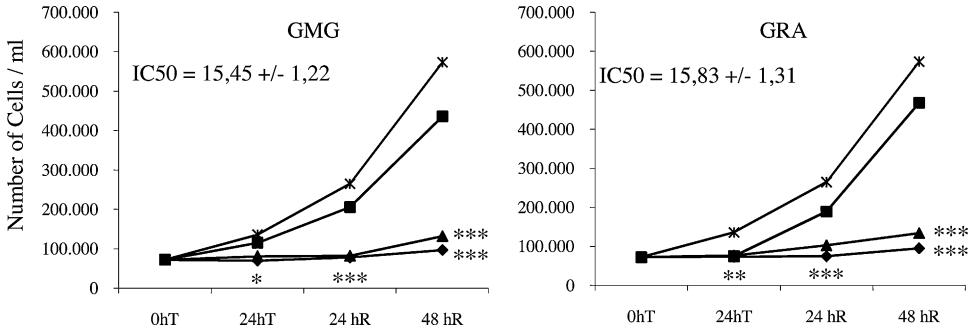

Fig. 6. Growth inhibition induced on HL60 cell by 24 h treatment with 10 (—■—), 20 (—▲—) and 30 μM (—●—) MA-GMG or MA-GRA. IC_{50} values were calculated 48 h after drug washout. Error bars represent the standard deviation. Statistical analysis: $^{*}p < 0.01$, $^{**}p < 0.005$, $^{***}p < 0.001$ compared with untreated controls.

cant starting from day 13, 3 days after the end of the treatment period. No toxicity was observed during the whole experimental period but, despite the reduced growth observed in treated mice, T/C values did not indicate a significant antitumoral activity with the best T/C value of 53.8%. In the second model, SCID mice bearing RPMI-8226 myeloma received either GMG-ITC or vehicle solution following the same schedule used in the former experiment. Mice receiving GMG-ITC showed a significantly slower tumor growth rate compared to controls starting from day 8 (Fig. 8, lower panel). Toxicity was not observed (max BWL = 7.8%) and T/C values demonstrated a statistically significant difference between the two groups with a best T/C of 33.9%. For this reason, treatment was continued into a 3rd week. At the end of the 3rd week GMG-ITC started to show toxicity with 2 out of 8 mice dying.

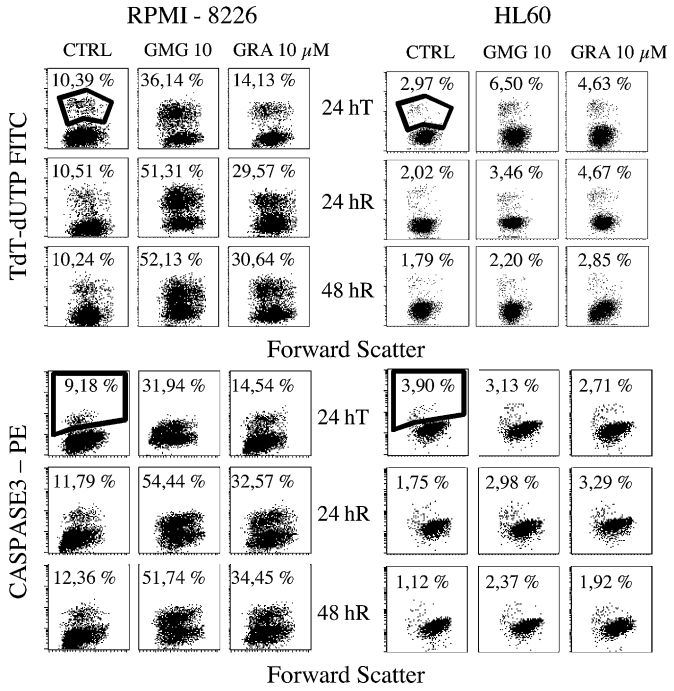

Fig. 7. Detection of apoptosis (upper panel): RPMI-8226 (left) and HL60 (right) cells were treated for 24 h with 10 μM of MA-GMG or MA-GRA. The biparametric TdT-d-UTP/Forward scatter flow cytometric analysis were performed after 24 h treatments and 24, 48 and 72 h after drug-washout. The percentage of apoptotic cells are also reported. Experiments were repeated three times with comparable results. Detection of active caspase-3 (lower panel): RPMI-8226 (left) and HL60 (right) cells were treated for 24 h with 10 μM of MA-GMG or MA-GRA. The biparametric caspase-3/forward scatter flow cytometric analysis were performed after 24 h treatment and 24, 48 and 72 h after drug-washout. The percentage of caspase-3 positive cells are also reported. Experiments were repeated three times with comparable results.

4. Discussion

GL-derived ITCs have been intensively studied in the last years due to their chemopreventive effects and, more recently, various studies demonstrated their potential use as novel chemotherapeutics [9,13,22]. GMG is an uncommon member of the GLs family and presents a unique characteristic consisting in a second saccaridic residue in its side chain. This GLs is a typical secondary metabolite present in vegetables belonging to the genus *Moringaceae* that consists of 14 species, among which *M. oleifera* is the most widely distributed. *M. oleifera* is a multipurpose tree which grows in many tropical or equatorial regions. The medical value of the seeds and other part of the plant have long been recognized in folk medicine [33]. The glycosylated ITC, resulting from myrosinase-hydrolysis of GMG, has been shown to exhibit a broad biological activity [33] and it was also shown to exert an effective antitumor activity [34]. GMG-ITC is a solid, odorless, and stable compound at room temperature that can be purified easily in high amounts differing from others natural bioactive ITCs which are

Day	T/C %
0	100
2	71,6
4	75,2
7	62,3
9	65,2
11	53,8
14	57,9
16	57,8
18	56,8
21	62,3

Day	T/C %
0	100
2	78,2
4	47,2
7	53,3
9	45,5
11	39,9
14	34,8
16	33,9
18	40,2
21	50,8

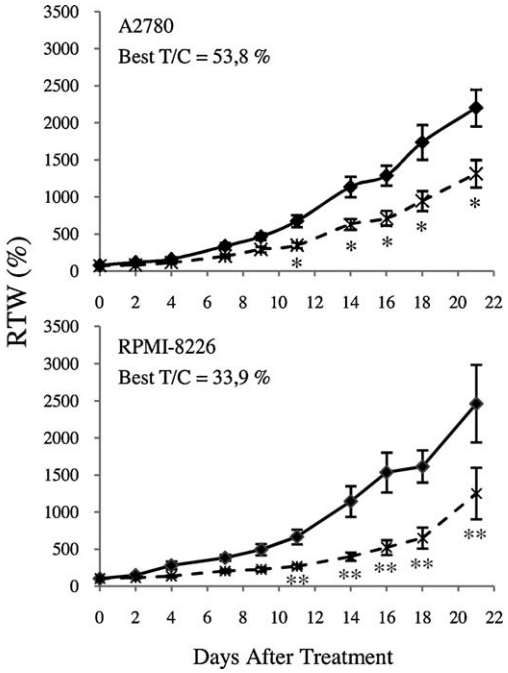

Fig. 8. Antitumoral activity of GMG-ITC on Swiss Ncr *nu*/*nu* mice bearing A2780 ovarian cancer (upper panel) or SCID mice bearing RPMI-8226 myeloma cancer (lower panel). Mice were treated with 20 mg/kg GMG-ITC i.p. once a day for 2 (*nu*/*nu* mice) or 3 (NUDE mice) weeks, 5 days a week. Result are shown as tumor weight of control (continuous line) and treated (crossed line) mice. Error bars represent the standard error. $^{*}p < 0.05$, $^{**}p < 0.01$ compared to control.

liquid, volatile, with pungent odors and usually present at lower concentrations. What we presented in this study represent the first data on this molecule and our findings demonstrate its potential use as a novel chemotherapeutic compound, expecially considering its overall increased potency compared to the most studied ITC, Sulforaphane. Our first experiments were aimed at determining the best time-exposure protocols and concentration range of activity of the two molecules in various human carcinoma cell lines, resulting in an optimal 24 h schedule of treatment at μM concentrations. The cell cycle analysis showed that both ITCs are unable to induce detectable cell cycle perturbations while still being able to significantly inhibit cell growth suggesting that in those cell lines, probably, ITCs do not activate a specific cell cycle checkpoint but slow down the progress of cells through all phases of cell cycle. Various studies have demonstrated that ITCs are able to induce phase-2 drug metabolizing enzymes and, among them, Glutathione-S-Transferase (GST) [14–17] has always been considered of great importance for these compounds to exert their effects. We investigated the ability of MA-GMG and MA-GRA to modulate GST-π activity in two isogenic cell lines (MCF7 π and NEO) with a 25 fold relative difference in GST-π basal activity. Our results suggest that, despite the partial influence shown by ITCs on the GST/GSH system, their cytotoxic effects are not as closely related to this. Both compounds, infact, did not show a significant increase in their potency even when coupled with the GSH depleting agent BSO (data not shown) despite being able to induce a 2.5–3.5 fold increase in its activity in MCF7 NEO cells. The NF-kB pathway is often associated with tumorigenesis when deregulated and, since it has been shown that ITCs can also modify the expression of various genes associated with inflammatory response [14–22], we decided to compare MA-GMG and MA-GRA effects on the expression of NF-kB and NF-kB dependant genes. Our experiments showed that both drugs were able to significantly downregulate NF-kB activity with MA-GMG showing a good dose-responsiveness with a peak of 70% inhibition at 30 μM and MA-GRA being less potent with a 30% inhibition peak. Due to the great importance of NF-kB related pathway in myeloma cells survival [30–32], we subsequently tested both compounds also on the RPMI-8226 human multiple myeloma cell line; both drugs showed an increased inhibitory effect in these cells with 40% inhibition already at 10 μM. Most noticeably, MA-GMG effect lasted up to 24 h after drug washout. In light of these results, we decided to perform also cell count assays and cell cycle analysis to better evaluate the potency of GL-derived ITCs on this type of malignant cells compared to carcinomas. Our experiments not only showed that both MA-GMG and MA-GRA were able to induce a stronger growth inhibitory effect and at lower doses (5–15 μM) but also that both drugs were able to induce long lasting cell cycle perturbations mostly consisting in G_2M accumulation. To highlight if this greater potency was due to the different heritage of myeloid-derived tumors compared to carcinomas, we performed the same experiments on the HL60 leukemia cell line. The results obtained demonstrated that this was not the case since HL60 cells did not show an increased sensitivity to MA-GMG or MA-GRA treatments compared to carcinoma cells, with a comparable IC_{50} of 15 μM. We also report here that both ITCs are able to induce caspase-3 dependant apoptosis in multiple myeloma cells but not in other myeloid nor carcinoma cells (data not shown). Even in this case MA-GMG showed a stronger and longer lasting effect when compared to MA-GRA. To confirm our *in vitro* data we finally performed a preliminary *in vivo* test comparing the activity of the purified GMG-ITC in two different mice models bearing either a carcinoma or a myeloma. As expected, GMG-ITC showed little activity in the carcinoma model reaching a best T/C value of 53.8% while, on the contrary, it was able to statistically affect the tumor growth rate in the myeloma model reaching a best T/C of 33.9% and maintaining a statistically significant activity for more than 14 days (from day 4th to day 18th). The mechanism of action of GL-derived ITCs still remains largely unknown but the results presented in this paper, showing an increased sensitivity of myeloma cells compared to carcinoma cells to ITC treatment both *in vitro* and *in vivo*, suggest that the inhibitory effects on NF-kB activity may play a key role in their activity considering that myelomas are known to strongly depend on NF-kB expression for their growth. Recently, the proteasome inhibitor Velcade was found effective on myelomas [35–37] and it was suggested that the reason for its specificity is linked to the reduced catabolism of IkB which, in turns, inhibit NF-kB activation. Multiple myeloma still remains one of the malignancies with the highest mortality and for this reason, despite new therapies with Velcade have improved the chances of survival for myeloma's patients, the need for new and improved drugs is still high. We envision the possibility that other drugs active on NF-kB inhibition, could have some potential for the treatment of myelomas and, in this respect, GL-derived ITCs could be possible candidates considering their relatively low toxicity. GMG-ITC seems to be a good candidate for further investigating ITCs potential in myeloma treatment since our results demonstrate that it is more potent than the commonly studied Sulforaphane and, in addition, it is easily extracted from the seeds of *M. oleifera* where it represents roughly 8–10% of the whole weight, thus making GMG one of the most available and probably also the most economic GL to obtain and purify.

Conflict of interest

Carla Manzotti and Carlo Morazzoni are employees of Indena S.p.A. who supported the study.

Acknowledgements

The generous contribution of the Italian Association for Cancer Research (AIRC) and Fondazione Mattioli to the Department of Oncology of Mario Negri Institute is greatly appreciated. This study was conducted with the financial support of Indena S.p.A.

Appendix A. Supplementary data

Supplementary data associated with this article can be found, in the online version, at doi:10.1016/j.bcp.2009.12.008.

References

[1] D'Incalci M, Steward WP, Gescher AJ. Use of cancer chemopreventive phytochemicals as antineoplastic agents. Lancet Oncol 2005;6(11):899–904.
[2] D'Incalci M, Brunelli D, Marangon E, Simone M, Tavecchio M, Gescher A, et al. Modulation of gene transcription by natural products—a viable anticancer strategy. Curr Pharm Des 2007;13(27):2744–50.
[3] Sidransky H, Ito N, Verney E. Influence of alpha-naphthyl-isothiocyanate on liver tumorigenesis in rats ingesting ethionine and N-2-fluorenylacetamide. J Natl Cancer Inst 1966;37(5):677–86.
[4] Fenwick GR, Heaney RK, Mullin WJ. Glucosinolates and their breakdown products in food and food plants. Crit Rev Food Sci Nutr 1983;18(2):123–201.
[5] Fahey JW, Zalcmann AT, Talalay P. The chemical diversity and distribution of glucosinolates and isothiocyanates among plants. Phytochemistry 2001; 56(1):5–51.
[6] Shapiro TA, Fahey JW, Wade KL, Stephenson KK, Talalay P. Human metabolism and excretion of cancer chemoprotective glucosinolates and isothiocyanates of cruciferous vegetables. Cancer Epidemiol Biomarkers Prev 1998;7(12): 1091–100.
[7] Getahun SM, Chung FL. Conversion of glucosinolates to isothiocyanates in humans after ingestion of cooked watercress. Cancer Epidemiol Biomarkers Prev 1999;8(5):447–51.
[8] Zhang Y, Talalay P. Anticarcinogenic activities of organic isothiocyanates: chemistry and mechanisms. Cancer Res 1994;54(7 Suppl.):1976–81.
[9] Hecht SS. Inhibition of carcinogenesis by isothiocyanates. Drug Metab Rev 2000;32(3–4):395–411.

[10] Conaway CC, Yang YM, Chung FL. Isothiocyanates as cancer chemopreventive agents: their biological activities and metabolism in rodents and humans. Curr Drug Metab 2002;3(3):233–55.
[11] Fowke JH, Chung FL, Jin F, Qi D, Cai Q, Conaway C, et al. Urinary isothiocyanate levels, brassica, and human breast cancer. Cancer Res 2003;63(14):3980–6.
[12] Zhao B, Seow A, Lee EJ, Poh WT, Teh M, Eng P, et al. Dietary isothiocyanates, glutathione S-transferase -M1, -T1 polymorphisms and lung cancer risk among Chinese women in Singapore. Cancer Epidemiol Biomarkers Prev 2001;10(10):1063–7.
[13] Conaway CC, Wang CX, Pittman B, Yang YM, Schwartz JE, Tian D, et al. Phenethyl isothiocyanate and sulforaphane and their N-acetylcysteine conjugates inhibit malignant progression of lung adenomas induced by tobacco carcinogens in A/J mice. Cancer Res 2005;65(18):8548–57.
[14] Steinkellner H, Rabot S, Freywald C, Nobis E, Scharf G, Chabicovsky M, et al. Effects of cruciferous vegetables and their constituents on drug metabolizing enzymes involved in the bioactivation of DNA-reactive dietary carcinogens. Mutat Res 2001;480–481:285–97.
[15] Talalay P, Fahey JW. Phytochemicals from cruciferous plants protect against cancer by modulating carcinogen metabolism. J Nutr 2001;131(11 Suppl.): 3027–33.
[16] Brooks JD, Paton VG, Vidanes G. Potent induction of phase 2 enzymes in human prostate cells by sulforaphane. Cancer Epidemiol Biomarkers Prev 2001; 10(9):949–54.
[17] McWalter GK, Higgins LG, McLellan LI, Henderson CJ, Song L, Thornalley PJ, et al. Transcription factor Nrf2 is essential for induction of NAD(P)H:quinone oxidoreductase 1, glutathione S-transferases, and glutamate cysteine ligase by broccoli seeds and isothiocyanates. J Nutr 2004;134(12 Suppl.):3499–506.
[18] Fimognari C, Nusse M, Cesari R, Iori R, Cantelli-Forti G, Hrelia P. Growth inhibition, cell-cycle arrest and apoptosis in human T-cell leukemia by the isothiocyanate sulforaphane. Carcinogenesis 2002;23(4):581–6.
[19] Bonnesen C, Eggleston IM, Hayes JD. Dietary indoles and isothiocyanates that are generated from cruciferous vegetables can both stimulate apoptosis and confer protection against DNA damage in human colon cell lines. Cancer Res 2001;61(16):6120–30.
[20] Srivastava SK, Singh SV. Cell cycle arrest, apoptosis induction and inhibition of nuclear factor kappa B activation in anti-proliferative activity of benzyl isothiocyanate against human pancreatic cancer cells. Carcinogenesis 2004; 25(9):1701–9.
[21] Xu C, Shen G, Chen C, Gelinas C, Kong AN. Suppression of NF-kappaB and NF-kappaB-regulated gene expression by sulforaphane and PEITC through IkappaBalpha, IKK pathway in human prostate cancer PC-3 cells. Oncogene 2005;24(28):4486–95.
[22] Heiss E, Herhaus C, Klimo K, Bartsch H, Gerhauser C. Nuclear factor kappa B is a molecular target for sulforaphane-mediated anti-inflammatory mechanisms. J Biol Chem 2001;276(34):32008–15.
[23] Barillari J, Gueyrard D, Rollin P, Iori R. Barbarea verna as a source of 2-phenylethyl glucosinolate, precursor of cancer chemopreventive phenylethyl isothiocyanate. Fitoterapia 2001;72(7):760–4.
[24] Barillari J, Canistro D, Paolini M, Ferroni F, Pedulli GF, Iori R, et al. Direct antioxidant activity of purified glucoerucin, the dietary secondary metabolite contained in rocket (*Eruca sativa* Mill.) seeds and sprouts. J Agric Food Chem 2005;53(7):2475–82.
[25] Pessina A, Thomas RM, Palmieri S, Luisi PL. An improved method for the purification of myrosinase and its physicochemical characterization. Arch Biochem Biophys 1990;280(2):383–9.
[26] Simone M, Erba E, Damia G, Vikhanskaya F, Di Francesco AM, Riccardi R, et al. Variolin B and its derivate deoxy-variolin B: new marine natural compounds with cyclin-dependent kinase inhibitor activity. Eur J Cancer 2005;41(15): 2366–77.
[27] Bertuzzi A, Gandolfi A, Germani A, Spanò M, Starace G, Vitelli R. Analysis of DNA synthesis rate of cultured cells from flow cytometric data. Cytometry 1984;5(6):619–28.
[28] Zhang Y. Role of glutathione in the accumulation of anticarcinogenic isothiocyanates and their glutathione conjugates by murine hepatoma cells. Carcinogenesis 2000;21(6):1175–82.
[29] Zhang Y, Talalay P. Mechanism of differential potencies of isothiocyanates as inducers of anticarcinogenic Phase 2 enzymes. Cancer Res 1998;58(20):4632–9.
[30] Ito K, Nakazato T, Xian MJ, Yamada T, Hozumi N, Murakami A, et al. 1′-Acetoxychavicol acetate is a novel nuclear factor kappaB inhibitor with significant activity against multiple myeloma in vitro and in vivo. Cancer Res 2005;65(10):4417–24.
[31] Yinjun L, Jie J, Yungui W. Triptolide inhibits transcription factor NF-kappaB and induces apoptosis of multiple myeloma cells. Leuk Res 2005;29(1):99–105.
[32] Feinman R, Koury J, Thames M, Barlogie B, Epstein J, Siegel DS. Role of NF-kappaB in the rescue of multiple myeloma cells from glucocorticoid-induced apoptosis by bcl-2. Blood 1999;93(9):3044–52.
[33] Anwar F, Latif S, Ashraf M, Gilani AH. *Moringa oleifera*: a food plant with multiple medicinal uses. Phytother Res 2007;21(1):17–25.
[34] Guevara AP, Vargas C, Sakurai H, Fujiwara Y, Hashimoto K, Maoka T, et al. An antitumor promoter from *Moringa oleifera*. Mutat Res 1999;440(2):181–8.
[35] Hideshima T, Richardson P, Chauhan D, Palombella VJ, Elliott PJ, Adams J, et al. The proteasome inhibitor PS-341 inhibits growth, induces apoptosis, and overcomes drug resistance in human multiple myeloma. Cells Cancer Res 2001;61(7):3071–6.
[36] LeBlanc R, Catley LP, Hideshima T, Lentzsch S, Mitsiades CS, Mitsiades N, et al. Proteasome inhibitor PS-341 inhibits human myeloma cell growth in vivo and prolongs survival in a murine model. Cancer Res 2002;62(17):4996–5000.
[37] Altun M, Galardy PJ, Shringarpure R, Hideshima T, LeBlanc R, Anderson KC, et al. Effects of PS-341 on the activity and composition of proteasomes in multiple myeloma cells. Cancer Res 2005;65(17):7896–901.